

# High resolution soft x-ray tomography in the Madison Symmetric Torus

P. Franz<sup>a)</sup>

*Consorzio RFX-Associazione EURATOM ENEA sulla fusione, Padova, Italy  
and Istituto Nazionale di Fisica della Materia, Unità di Ricerca di Padova, Italy*

F. Bonomo, G. Gadani, and L. Marrelli

*Consorzio RFX-Associazione EURATOM ENEA sulla fusione, Padova, Italy*

P. Martin and P. Piovesan

*Consorzio RFX-Associazione EURATOM ENEA sulla fusione, Padova, Italy  
and Istituto Nazionale di Fisica della Materia, Unità di Ricerca di Padova, Italy*

G. Spizzo

*Consorzio RFX-Associazione EURATOM ENEA sulla fusione, Padova, Italy*

B. E. Chapman and M. Reyfman

*MST Group, Physics Department, University of Wisconsin, Madison, Wisconsin 53706*

(Presented on 21 April 2004; published 12 October 2004)

We present in this article the description of the upgraded soft x-ray tomographic diagnostic which has been installed in the Madison symmetric torus (MST) reversed field pinch. The previous diagnostic has been extended with two manipulators, for a total of three moveable probes and a fixed one. The line integrated emissivity (brightness) will be measured with arrays of photodiodes and the total number of channels has been increased from 24 to 74. The electronic layout has also been upgraded, and a type of custom made current-to-voltage amplifier has been developed. The diagnostic will be used to continue and extend the magnetohydrodynamics analysis of the MST plasma. The imaging of rotating coherent structures (one or, as recently showed, two) which appear during quasisingle helicity or pulsed poloidal current drive experiments will be performed in more detail. The photocameras can be easily extracted, modified, and inserted again, allowing applications and utilizations of the diagnostic. © 2004 American Institute of Physics. [DOI: 10.1063/1.1794845]

## I. INTRODUCTION

During the years 2001–2003 a soft x-ray (SXR) tomographic diagnostic<sup>1</sup> has been installed and operated in the Madison Symmetric Torus (MST) reversed field pinch (RFP).<sup>2</sup> The diagnostic was composed by two miniaturized probes (photocameras), each camera housing a linear array of silicon photodiodes measuring the SXR radiation emitted by the plasma along a total of 24 lines of sight.

This experimental setup, used in different plasma conditions, has produced very interesting results, the main one being the detecting of rotating coherent structures, that is locally enhanced SXR emissivity regions, in the core of the plasma.<sup>3</sup> These coherent structures, in the hypothesis of correspondence between constant SXR emission and constant flux surfaces, are directly linked to the core magnetic topology of the RFP. When the spectrum of  $m=1$  modes condenses spontaneously to one dominant mode with a well-defined toroidal number  $n$  [these spectra are referred to as the quasisingle helicity state<sup>4</sup>], a SXR structure, hotter than the plasma nearby, is detected in the plasma core. In fact, this SXR region can be strongly correlated with the dominant magnetic mode. In particular in MST, thanks to magnetic modes rotation, fluctuation analysis and tomographic reconstruction allow for this identification. The SXR structure is

observed to rotate at exactly the same frequency as the poloidal phase of the dominant mode. In addition, the position of the SXR region corresponds to the island O-point (in other words the position of the SXR structures as tomographically reconstructed corresponds to the poloidal phase of the modes). Finally, the radial positions of SXR structures corresponding to dominant  $m=1$  modes with different helicities (different  $n$ , for example 5, 6, or more) are consistent with the positions of the modes given by the safety factor profile  $q(r)$ . A further result consists in multiple SXR structures observed in the MST plasma during a current profile control experiment [pulsed poloidal current drive<sup>5</sup>]. In fact, when mode amplitudes are small and stationary for a sufficiently long period, two rotating regions, corresponding to two different  $m=1$  modes, exist simultaneously in the plasma.

All of the experimental evidences presented so far have been interpreted as a consequence of a reduction and eventually of the disappearance of magnetic chaos inside the core region of the MST plasma. Given the importance of these results, the tomographic diagnostic has been upgraded in order to resolve these SXR structures and the plasma magnetic topology in higher details. In particular, two SXR photocameras have been recently installed in MST, increasing the number of available probes from the existing two to four. This upgrade has augmented the number of lines of sight

<sup>a)</sup>Electronic mail: paolo.franz@igi.cnr.it

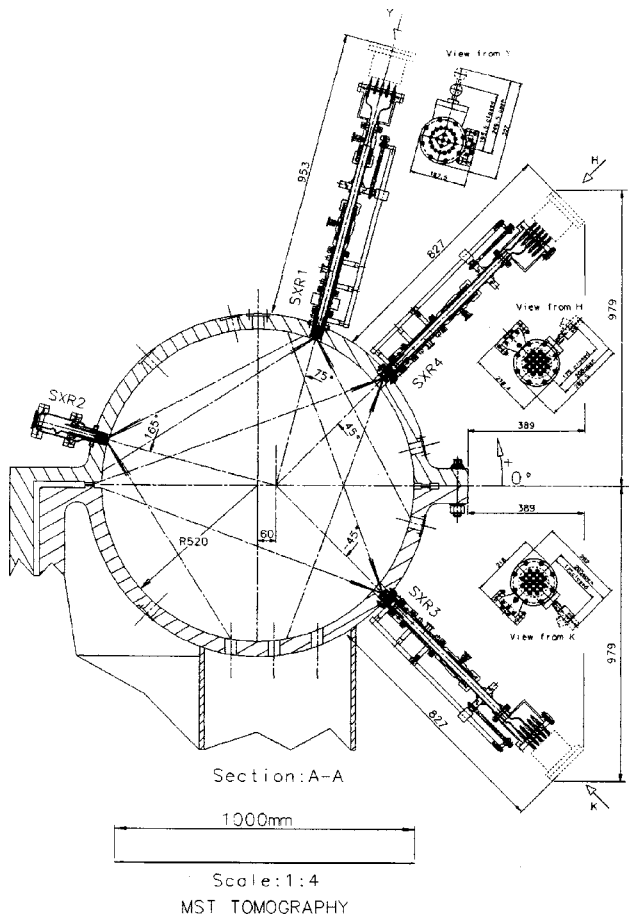


FIG. 1. Layout of the tomographic diagnostic. View of the four probes in the poloidal section of MST.

from 24 to 74, and the chords are better distributed, improving the coverage in the poloidal section. All this will increase the spatial resolution of the diagnostic.

This article will describe the tomographic system. Section II will illustrate in detail the probes. Future and applications of the upgraded diagnostic will be the subject of Sec. III.

## II. DESCRIPTION OF THE DIAGNOSTIC

The tomographic system of MST is composed of four units, labeled SXR1 to SXR4; see Fig. 1 for a layout of the diagnostic. All the probes are installed on 1.5 in. portholes of the MST vacuum vessel, in the same toroidal location. In particular, the SXR1 probe (located at 75 deg poloidal) is mounted in a manipulator, which enables one to insert, extract, or move the diagnostic. The SXR2 (at 165 deg) is more compact and place the SXR probe in a fixed position. These are the devices previously installed in MST. The instruments, SXR3 and SXR4, are very similar to the SXR1 one: the probes are mounted on manipulators and are located at 315 and 45 deg, respectively.

All the instruments can be divided in two subsystems, the photocamera, which contains the detectors, and the mechanical support, used to place the SXR photocamera in its operating position.

The photocamera is an aluminum cylinder, diameter = 35 mm, closed by an aluminum disk on one side (which is the part exposed to the plasma) and attached to a metal tube on the other.

An array of 20 silicon photodiodes, mounted on a teflon socket, is installed inside the camera. The photodiodes act as radiation-current converters, with the output current proportional to the energy of the SXR photons striking the detectors (3.6 eV are required to generate an electron-hole couple). The array used in all the photocameras is the AXUV-20ELM 20 diodes array manufactured by International Radiation Detectors, Inc., Torrance, CA<sup>6</sup> (the “M” stands for a modified version of the array chip with smoothed corners, ordered for compatibility with the photocamera dimensions). The diodes (in a common anode configuration) are  $0.75 \times 4$  mm with an active thickness of 35  $\mu\text{m}$ , and are used without bias voltage (absorption of photons is up to 6–7 keV).

The front aluminum disk contains a small slit (pinhole) and a beryllium foil. The pinhole ( $1 \times 4$  mm for all cameras) is used to define the geometry of the lines of sight. Figure 2 shows the chords of the SXR photocameras [Fig. 2(a) for the SXR1 and SXR2, and (b) for the other probes]; Fig. 2(c) shows the coverage of the  $p$ - $\phi$  space. Four fans of lines of sight are defined, with a total number of 74 chords: 20 each for SXR1, SXR3, and SXR4, and 14 for SXR2. The recent probes, in particular, use all the 20 diodes of the array, while the SXR2 probe was designed to consider every second detector, with six consecutive diodes only in the center of the fan. The distance between the array of detectors and the pinhole defines the actual angular aperture of the set of chords. When the front disk is mounted on the probe this distance is 10 mm. SXR1 and SXR2 have been used, and will be still used in this condition. By putting small aluminum rings (appropriately designed) between the probe and the front disk, the distance pinhole-detectors can be increased. As a consequence, the angular aperture of the fan of lines of sight will be reduced and the chords will be closer to each other. Thus, two rings 5 mm long have been installed in the SXR3 and SXR4 photocameras, with a total distance of 15 mm, to enhance the resolution in the core of the plasma (where the SXR structures mostly appears), and to allow for a better sampling of the emissivity distribution. This distance cannot be increased further (for example to 20 mm) as the SXR structures with higher radius ( $m=1$ ,  $n=7$ ) can be out of the fan of lines of sight during its rotation.

A thin beryllium foil is placed on the front disk, between the pinhole and photodiodes, and acts as high pass energy filter to select only the SXR radiation and to stop the visible light. The thicknesses of the foils have been carefully selected, and are all in the range 13–14  $\mu\text{m}$  (which corresponds to a cutoff energy of about 1 keV; 1  $\mu\text{m}$  of tolerance in the thickness is not relevant for our measurements). The photocameras are all equipped with curved Be foils, included in an arc frame, and all of the lines of sight are perpendicular to the surface of the absorber. One problem which can arise is the progressive coating of the foil with impurities (mainly carbon) as it remains exposed to the plasma. In fact, during the previous experimental campaigns, we found that after a few months of operation the foils were slightly blackened,

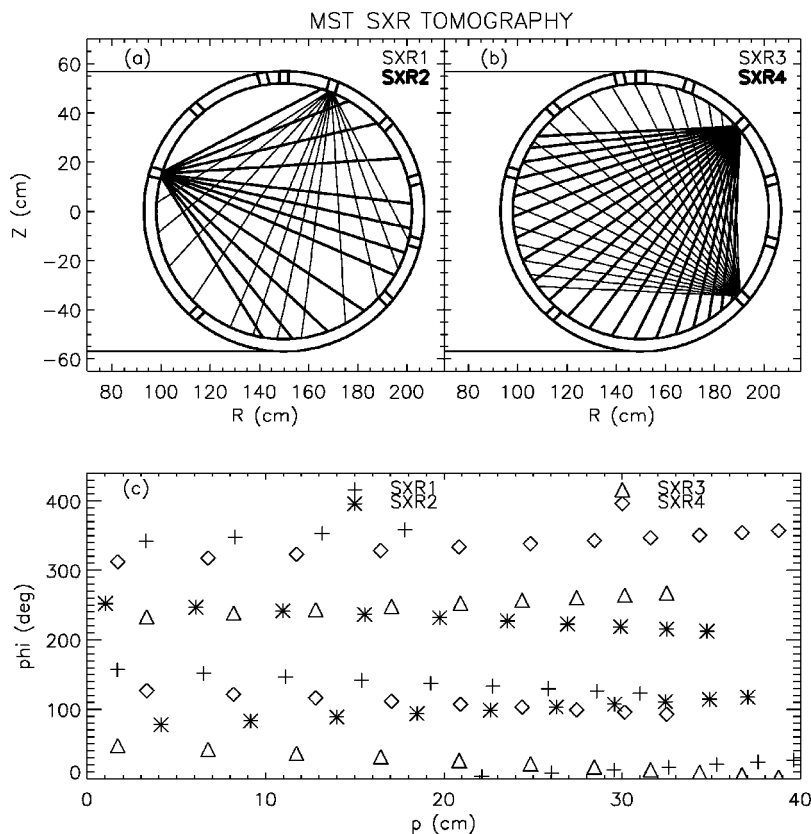


FIG. 2. Lines of sight of SXR1, SXR2 (a) and SXR3, SXR4 (b). Graph (c) of the chords in the  $p$ - $\phi$  plane ( $p$  is the perpendicular distances from the lines to the origin,  $\phi$  is the angle of this perpendicular with the equatorial plane).

and the coating was not uniform on the foil surface. We believe that this nonuniformity is due to the particular way the magnetic field lines end on the foil. To avoid this (Be foils can be expensive, and it can be difficult to find them with the same thickness) and to protect the photocameras, the probes measuring position (the distance of the pinhole from the inner wall of the vacuum vessel) will be 30 mm, instead of the 10 mm of the SXR1 and SXR2 probes. In addition, to increase protection, the probes have been placed on manipulators, so that they remain inserted only during the experimental session, and are extracted in all days when the SXR data are not needed. The SXR2 probe is fixed in its position, so that a periodical check and replacement of the Be foil will be done (which will require a planned vent of the machine).

The actual geometry of the lines of sight of the probes as well as design parameters (such as the pinhole dimension, the separation between pinhole and detectors, and the absolute position of the probes) have been studied with a complete set of simulations of the measurements. A SXR emissivity model have been defined, depending on the electron temperature and density profiles (impurities contributions have not been taken into account). In particular, the occurring of SXR structures in the plasma has been simulated through a local increase of the temperature. The experimental measurements (brightness) have been reproduced as much closely as possible, and examples of various SXR structures at different poloidal location have been simulated. The variations of the emissivity perpendicularly to the lines of sight have been considered in the calculations: The finite dimensions of the pinhole and detector actually defines a "cone of sight" (solid angle), and not a simple line. When these cones

are large enough, the emissivity could not be constant in the transverse direction to the line, and this, if not taken into account, could give nonrealistic results. This model has permitted us to study many different possible geometries, and allowed us to calculate the optimum values for the mentioned parameters. Moreover, the simulations have selected the (45,315) degree poloidal portholes as the best location to improve the tomographic diagnostic.

As previously stated, the SXR photocameras are placed in position by a support system, which can be a manipulator or a fixed support. The SXR1 diagnostic, together with the new ones, SXR3 and SXR4, are all manipulators. Figure 3 shows one manipulator (SXR3). The flexibility given by this type of mechanical support is an important feature, and revealed necessary also for extracting the probes when not in

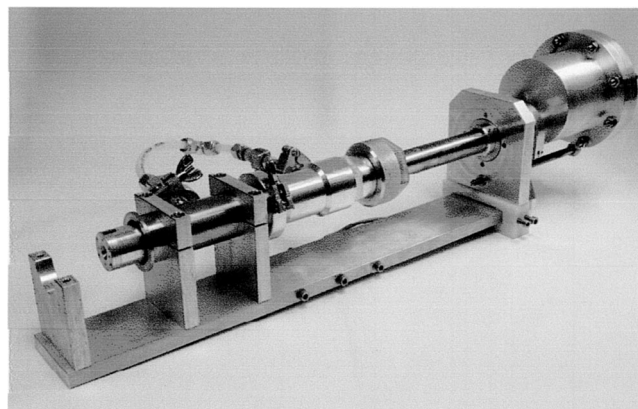


FIG. 3. Picture of one manipulator. The photocamera is the small cylinder in the left side of the picture.

use. The cameras can also be rotated or in general moved to other positions, allowing different configurations of lines of sight to be explored. A gate valve is used to decouple the probe from the vacuum of MST, and to screen it from the plasma. The manipulators are 10 cm shorter and have a faster insertion/extraction system than the one of SXR1. SXR2, on the other hand, has been installed on the fixed version of the support subsystem, which inserts the photocamera in a permanent position, without any valve, directly connected to the vacuum of the machine. In both types the probes are attached to a tube which contains the signal cables. All the signals are then extracted in a rear flange using vacuum feedthrough. In particular, three diagnostics use bipolar connectors, while the SXR1 uses an old-type unipolar feedthrough (we are planning to replace the flange in this diagnostic and install the same type of bipolar connectors).

The common anode configuration of the photodiodes array has been carefully studied and finally the optimal grounding layout has been designed. In this case the circuit has been grounded directly on the array socket, through small wires connected to the metal housing and to the MST vessel. The detectors can be, in fact, very sensitive to pickup noise but we found that this configuration significantly reduces this noise.

The output currents of the diodes (in the range of 20 nA to 5–10  $\mu$ A) will be processed through current-to-voltage amplifiers. Both commercial and custom made transimpedance linear amplifiers will be used, with bandwidth ranging between 10 kHz (edge chords) and a few hundreds kHz (for the lines of sight looking at the core of the plasma). The electronic layout has also been upgraded. A custom encoder system has been produced, which allows one to record the amplifier gain in the digitized signals. A circuit has been built that provides a pulse of different voltage (height) depending on the gain. The pulse is short (500  $\mu$ s), and it can be added to the amplified signals with each plasma (and before each plasma begins). Thus, one can tell easily what gain has been set for each channel by looking at the digitized signal. Different types of amplifiers have been developed, and are presently under investigation. One is made of a cascade of a translinear and a 160 db logarithmic stage, which should help in increasing the dynamic range of the signals. The other is a miniaturized, 20 channel, preamplifier to be installed right behind the detector. In this case the electronic noise should be reduced to a very low level due to the absence of cables between the photodiodes and the amplifiers, and should preserve the frequency response of the measured signals. The signals will be then digitized in CAMAC-type digitizers (16 channels per unit, 12 bit resolution) with a sampling rate variable between 1 and 10 MS/m. To further

reduce noise an isolated amplifier stage (gain 1) has been installed between the output of the amplifier and the input of the digitizer.

### III. APPLICATIONS

The final instrument will be composed by three moveable probes and a fixed one. The line integrated emissivity (brightness) will be measured with four fans of lines of sight, and the total number of channels will be 74. The diagnostic will be used to continue and extend the MHD analysis of the MST plasma. In particular the imaging and the topological description of rotating coherent structures (one or, as recently showed, two) which appear during quasisingle helicity or pulsed poloidal current drive experiments can be performed in more detail, and the complete evolution of these islands (associated with one or two  $m=1$  magnetic tearing modes) can be followed. In addition, in order to analyze the propagation of heat pulses, which can be followed as they travel across the plasma, a different pinhole can be installed in one or more probes to increase the poloidal coverage at the edge, where these events occur. The possibility of insertion and extraction of the photodiode arrays, and the special design of the photocameras, will permit applications. A very interesting one is the possibility to measure the 2- $d$  electron temperature profile using the double filter technique<sup>7</sup> taking the ratio of two tomographic reconstructions of the SXR emissivity, one obtained with the SXR1, SXR2 probes and a Be thickness and the other with the SXR3, SXR4 cameras and a different Be foil. Using two probes instead of four will provide less resolved reconstructions, but will have the advantage to allow one to analyze the fast variation of the temperature in the core of the plasma. This SXR data, also, will allow a test of a version of the Cormack-Bessel tomographic reconstruction algorithm<sup>8</sup> we are presently studying, modified to take into account the solid angle subtended by each of the diodes.

### ACKNOWLEDGMENTS

The RFX authors would like to thank I. Molon for the skilful technical help in the design and realization of the cabling of the probes and all the RFX team. S. C. Prager, J. S. Sarff, and all the MST team are also greatly acknowledged.

<sup>1</sup>P. Franz *et al.*, Rev. Sci. Instrum. **74**, 2152 (2003).

<sup>2</sup>R. N. Dexter *et al.*, Fusion Technol. **19**, 131 (1991).

<sup>3</sup>P. Franz, L. Marrelli, P. Piovesan *et al.*, Phys. Rev. Lett. **92**, 125001 (2004).

<sup>4</sup>L. Marrelli, P. Martin, G. Spizzo, P. Franz *et al.*, Phys. Plasmas **9**, 2868 (2002).

<sup>5</sup>J. S. Sarff, *et al.*, Nucl. Fusion **43**, 1684 (2003).

<sup>6</sup>International Radiation Detectors Inc., 2575 West, 237th Street Unit C, Torrance, CA 90505-5243, <http://www.ird-inc.com>

<sup>7</sup>R. Bartiromo, L. Carraro, P. Franz *et al.*, Plasma Phys. Controlled Fusion **42**, 881 (2000)

<sup>8</sup>P. Franz *et al.*, Nucl. Fusion **41**, 695 (2001).